

Dye–surfactant interaction: solubilization of styryl pyridinium dyes of varying alkyl chain in alfa-olefinic sulfonate and linear alkyl benzene sulfonate solutions

P.K. Behera^{a,*}, S. Mohapatra^a, S. Patel^b, B.K. Mishra^{b,1}

^a Photochemistry Research Group, Department of Chemistry, Sambalpur University, Jyoti Vihar, Sambalpur 768019, India

^b Centre of Studies in Surface Science and Technology, Department of Chemistry, Sambalpur University, Jyoti Vihar, Sambalpur 768019, India

Received 31 October 2003; received in revised form 16 June 2004; accepted 6 July 2004

Available online 17 August 2004

Abstract

Cationic dyes, like alkyl styryl pyridinium dyes, are found to interact with anionic surfactant systems differently according to their structural differences. The absorption and emission spectral data of the dyes in various organic solvents and in a wide range of surfactant concentration reveal a variation in the solubilization pattern of the dyes with varying alkyl chain at the pyridinium end. The existence of monomer and H/J-stacked dimers in aqueous medium as well as in surfactant media gets evidence from the spectral data. The difference in binding constant of the dyes with the surfactant aggregates is rationalized through the change in hydrophobicity of the dye due to change in alkyl chain.

© 2004 Published by Elsevier B.V.

Keywords: Styryl pyridinium dyes; Slippage; H/J-stacking; AOS; LABS

1. Introduction

One of the most fundamental properties of aqueous micellar solution is their ability to solubilize a wide variety of organic solutes with quite distinct polarities and degree of hydrophobicity. The self-association of dyes in solution and at interfaces due to strongly attractive van der Waal forces is a well-known phenomenon. The aggregation leads to a strong coupling of the molecular transition dipole moments, resulting in a narrow excitonic absorption band, which is considerably shifted in wavelength from the absorption of the monomeric species. Aggregates, which exhibit a red shift, are termed J-aggregates, and those, which have a blue shift, are referred to as H-aggregates [1–3]. Emerson et al. [4] have claimed to show the first electron micrographs of an H-aggregate and have given an interpretation of the phe-

nomenon of hypsochromism (blue shift) and bathochromism (red shift) resulting from the formation of H-aggregation and J-aggregation, respectively, by using a molecular exciton model. Thus, as illustrated in Scheme 1 for a stack-like aggregate, the transition intensity accumulates in the long wavelength transition for a tilt angle α (angle between the long axis of individual molecules and the line of centers in the aggregate) of $<32^\circ$, i.e. a J-aggregate structure. For tilt angle greater than this value (approaching 90°) the intensity builds up in the short-wave transition and the H-aggregate band appears.

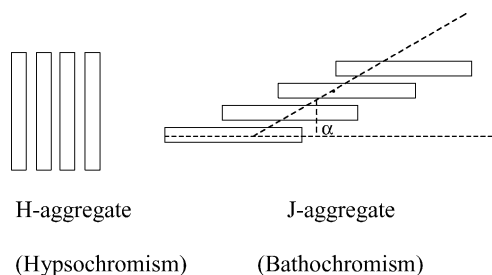
The photophysical and photochemical properties of J-aggregates have also attracted attention recently because of their potential as laser materials, in molecular electronics, and in displays and non-linear optical devices [5] and because of their analogous characteristics to aggregates having importance in biology, such as those in photosynthetic systems.

We have recently reported the hydrophobic contributions of the styryl pyridinium dyes in dye–surfactant interaction by using homologous series of solutes possessing the same

* Corresponding author. Tel.: +91 663 2430356; fax: +91 663 2430158.

E-mail address: pradiptabehera@rediffmail.com (P.K. Behera).

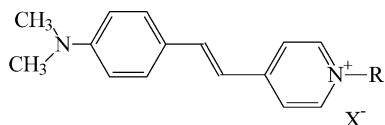
¹ Co-corresponding author.



Scheme 1. Schematic diagrams of H-aggregate and J-aggregate.

polar moiety but differing in the length of the attached alkyl chains within a given surfactant micelle [6–9]. Unlike homogeneous solvents, micelles possess a gamut of solubilization environment ranging from the non-polar hydrocarbon core of the micelle to the relatively polar micellar–water interface. This inherent microheterogeneity of micellar environment can play an important role in determining the nature of relative abundance of various factors that contribute to solubilization [10–11]. Not only the structure of the solute but also the structure of the surfactant, that builds the micelle, contributes to the localization of the solute within the micelle.

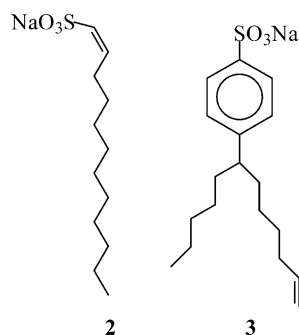
In this paper, we report on the spectral and photophysical properties of a series of styryl pyridinium dyes (**1**) with varying hydrophobicity in two structurally different industrially important anionic surfactants, alfa-olefinic sulfonate (AOS, **2**), linear alkyl benzene sulfonate (LABS, **3**).



R = C_nH_{2n+1} (n = 1, 3, 5, 6, 8, 10, 12, 14, 16 and 18)

X = Br and I.

(1)



2

3

2. Experimental

2.1. Materials

N-alkyl-4-(p-N,N-dimethylamino styryl)pyridinium bromides (**1**) were prepared by the method reported earlier

Table 1

The absorption and emission data of three representative dyes with n = 3, 10 and 16 in various organic solvents

Sl. no.	Solvents	C ₃		C ₁₀		C ₁₆	
		λ _{max}	λ _{em}	λ _{max}	λ _{em}	λ _{max}	λ _{em}
1	Ethylene glycol	482	582	482	582	483	582
2	Methanol	479	579	479	579	478	576
3	Ethanol	484	576	484	577	484	578
4	Butanol-1	490	576	490	576	489	576
5	Isobutanol	491	573	491	572	491	573
6	Cyclohexanol	492	571	492	571	494	571
7	Butanol-2	489	573	489	573	489	573
8	Acetonitrile	474	555	474	556	474	585
9	DMSO	476	589	475	589	476	589
10	DMF	474	587	473	587	474	587
11	DMA	474	587	474	586	474	587
12	Acetone	476	586	476	586	477	586
13	Pyridine	494	589	494	590	496	590
14	Chloroform	492	571	495	560	496	560
15	Dioxane	463	557	464	555	463	554
16	Benzene	477	552	477	550	477	550

[12–13]. The dyes are referred to as C_n according to the number (n) of carbon atom in the alkyl chain (**1**). AOS and LABS were from SMZS Chemicals Ltd., Pune and were used without further purification. Triple distilled water was used throughout the experiment.

2.2. Spectroscopic measurements

A concentrated (ca. 1 mM/l) stock solution of each dye was prepared separately by dissolving the required amount of the dye in methanol. The solution for spectral measurement was prepared by adding 0.1 ml of the stock solution to a 5 ml volumetric flask containing freshly prepared solution of the surfactant in triply distilled water. Aliquots of these solutions were added to a quartz cuvette thermostated at 25 °C. Absorption spectra were recorded on Shimadzu-160 A spectrophotometer and emission spectra were recorded on a Shimadzu-RF5000 spectrofluorophotometer.

3. Results and discussion

The absorption and emission spectra of C₁–C₁₈ dyes have been studied in polar (2% MeOH–H₂O, v/v) and in microheterogeneous (anionic AOS and LABS micelles) media. The data of absorption and emission spectra of three representative dyes with n = 3, 10 and 16 in various organic solvents have been reported in Table 1. Without the presence of surfactants in methanol–H₂O medium and in organic solvents, the change in alkyl chain attached to the pyridinium nucleus does not have any effect on the absorption and emission maxima.

3.1. Absorption spectra

In the visible region, all the dyes except C₁₆ and C₁₈ absorb at 450–457 nm in the absence of surfactant. Both C₁₆ and

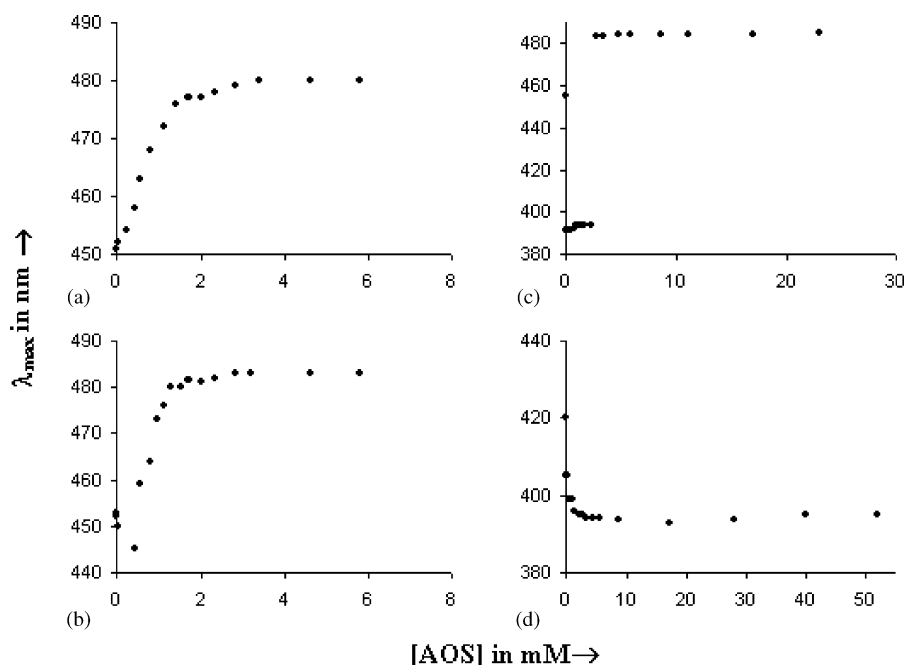


Fig. 1. Plot of [AOS] vs. λ_{\max} of: (a) C₃-NMe₂; (b) C₈-NMe₂; (c) C₁₂-NMe₂ and (d) C₁₈-NMe₂ dyes.

Table 2
The CMC values in the presence of different dyes as probes

Sl. no.	Dye	Break point (CMC)
1	C ₁	1.500
2	C ₃	1.125
3	C ₅	1.125
4	C ₆	1.125
5	C ₈	1.125
6	C ₁₀	0.937

C₁₈ dyes exhibit peaks at 475 and 416 nm with shoulders at 400 nm. Behera and co-workers [14] have assigned the peaks at 400 and 475 nm to the dimer and monomer of the dyes, respectively.

3.1.1. In presence of AOS

On addition of AOS, the absorption maxima of the dyes (C₁–C₁₀) are found to increase with increasing concentration of the AOS till a plateau is obtained in the plot of λ_{\max} versus [AOS] (Fig. 1). The onset of the plateau in the plot of λ_{\max} versus [AOS] may be due to the aggregation of the surfactant to form the micelle, which may be considered as the critical micelle concentration (CMC) of the surfactant in aqueous medium. The CMC values in the presence of different dyes as probes are given in Table 2. The average value of CMC is obtained to be 1.2 ± 0.3 mM.

On addition of AOS, a broad peak centering around 480 nm is obtained with a shoulder at 391 nm for C₁₂–C₁₈ dyes, which is not observed for dyes with shorter chain length. The shoulder at 391 nm may be assigned to the dimers formed due to the assistance of surfactant chain. Mishra et al. [15] have also reported a surfactant-assisted dimerization of C₁₆

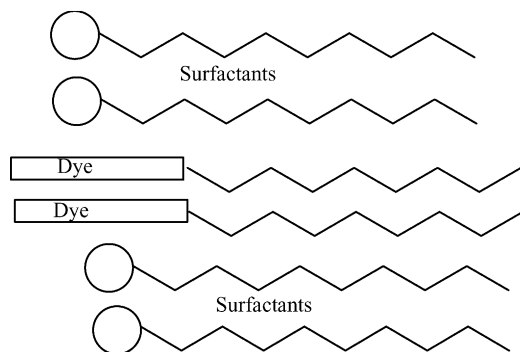
dye in the presence of cetyltrimethyl ammonium bromide. The dimerization leads to a stacking phenomenon of the chromophoric group such that the p-orbitals of the chromophores overlap and in consequence there is a large hypsochromic shift from that of the monomer species. For C₁₂ dye, the shoulder appears at 391 nm up to 1.73 mM of AOS. For C₁₄ and C₁₆ dyes the same transition leads to a peak up to 4.63 and 17 mM of AOS and then to a shoulder up to 17 and 46 mM of AOS, respectively. However, for C₁₈ dye the species relating to 391 nm peak exists along with the monomeric species (475 nm) throughout the experimental concentration of AOS. The ratios of dimer to monomer with respect to [AOS] for C₁₂–C₁₈ dyes are given in Table 3. The analysis of data of Table 3 suggests that with increasing hydrophobicity in the dyes, the population of the dimeric species increases. The order of increasing population of dimeric form of dyes is C₁₂ < C₁₄ < C₁₆ < C₁₈.

Within 0.01–0.34 mM of [AOS] the solution becomes turbid for C₆–C₁₀ dyes. The appearance of turbidity may be attributed to the charge neutralization of the species ([Dye] = 0.02 mM) in the presence of anionic surfactants. The turbidity range does not depend on the chain length of the dye. In the turbidity zone, C₆ dye absorbs at 457–459 nm with a broad band, which indicates, essentially, no change in the environment of the dye chromophore. For C₈ and C₁₀ dyes peak broadening appears at 418–421 nm. These peaks disappear beyond 0.34 mM for C₈ and 0.58 mM for C₁₀ dyes. For C₁₀ dye, the 421 nm band persists (up to 0.58 mM of AOS) even after the disappearance of the turbidity. This broad band around 418–421 nm may be attributed to dimerization leading to H-type aggregation of the dye molecules assisted by the surfactant chain (Scheme 2) in a relatively more polar than water.

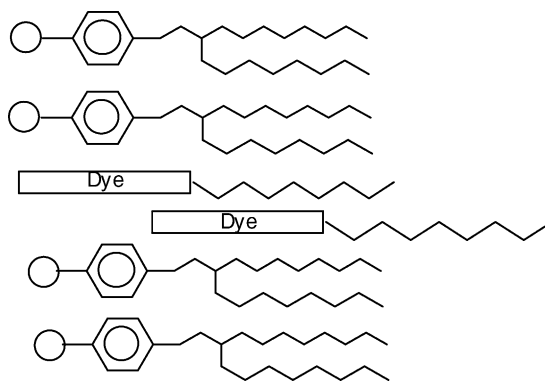
Table 3
The ratio of dimer to monomer with respect to [AOS] for C₁₂–C₁₈ dyes

[AOS] (mM)	Ratio of dimer to monomer			
	C ₁₂	C ₁₄	C ₁₆	C ₁₈
0.057	–	1.58	1.78	2.49
0.11	–	1.66	2.38	–
0.23	–	1.95	–	2.41
0.34	–	2.22	2.57	–
0.58	–	2.21	2.48	2.61
0.80	0.57	2.57	–	–
1.30	0.34	2.98	–	–
1.56	0.38	–	–	2.89
1.73	0.27	2.94	–	–
2.31	–	2.49	–	2.97
2.80	–	2.14	–	2.89
3.40	–	1.77	–	2.84
4.63	–	1.05	2.30	2.80
5.80	–	0.83	2.29	2.75
8.60	–	0.60	1.85	2.77
11.0	–	0.50	–	–
17.0	–	0.29	–	2.48
28.0	–	–	0.73	2.07
40.0	–	–	0.39	1.78
52.0	–	–	0.33	1.27

The shifts in the λ_{\max} from zero [AOS] to 5.8 mM [AOS] are 23, 29 and 32 nm for C₁, C₃ and C₅ dyes, respectively. Comparing with the λ_{\max} values in various solvents (Table 1), it can be proposed that, the solubilization sites for C₁ and C₅ dyes are the outer and inner regions of the interface, respectively, and C₃ dye occupies a site in between these two regions. After complete micellization ([AOS] > 1.2) the λ_{\max} of C₆–C₁₀ dyes are found to be the same as that of C₅ dye. With increasing [AOS], the λ_{\max} values increase to 485 nm for C₁₂–C₁₆ dyes. In this condition, the peak due to dimer (391 species) is not observed. This observation may infer that C₁₂, C₁₄ and C₁₆ dyes occupy slightly inner core of the micelle with respect to the dyes having shorter alkyl chain. However, for C₁₈ dye the plot of λ_{\max} versus [AOS] is found to be asymptotic (Fig. 1(d)). The λ_{\max} value immediately falls from 420 to 395 nm at 2.3 mM of AOS and then remains constant. It clearly suggests that the dimer of C₁₈ dye remains at



Scheme 2. Schematic representation of plane-to-plane staking of dyes to form an H-aggregate.



Scheme 3. Schematic representation of end-to-end staking of dyes to form a J-aggregate.

bulk phase throughout the [AOS]. The appearance of a shoulder at 475 nm is indicative of the existence of monomer in aqueous as well as micellar media.

3.1.2. In presence of LABS

The plots of λ_{\max} versus [LABS] are shown in Fig. 2. The dotted line in the lower concentration range of the surfactant in the rising arm for C₁–C₈ dyes represents the turbid zone. At higher concentration range, the plot exhibits a plateau almost parallel to the X-axis. The constancy in the λ_{\max} values in this concentration range is an indication of saturation in the solubilization of the dyes in the surfactant aggregates. The rising arm of the plot delineates the transition during compartmentalization of the dye between bulk and surfactant aggregates. The absorption spectra of C₁–C₁₀ dyes do not show any characteristic peak of dimer throughout the experimental condition. However, in the turbid region, a broad peak is observed around 550 nm. While studying the spectral behaviour of C₁₆ dye in CTAB reversed micelle, Mishra et al. [15] have observed a shoulder at 510 nm and have attributed the absorption to J-type of aggregation of the dye at the micelle–water interface. The absorption at 550 nm, in the present study, may also be rationalized by proposing a J-type of aggregation, which may be assisted by the organization of the surfactant (LABS) (Scheme 3).

For C₁₂ and C₁₄ dyes the monomers in aqueous medium form dimer immediately after the addition of the surfactant leading to a hypsochromic shift up to 420 nm. At higher concentration than CMC, for C₁₂–C₁₈ dyes, the dimers solubilize in the surfactant aggregates as monomers experiencing similar absorption characteristics as that of C₁–C₁₀ dyes. However, for C₁₆ and C₁₈ dyes, the peaks for dimers are found to be retained after the addition of surfactant up to a certain concentration (1.44 mM) and then at higher concentration of surfactant these dyes are found to be solubilized in the micelle as monomer.

On addition of LABS a narrow turbidity zone is observed for C₁–C₁₀ dyes at low concentration of LABS. The turbidity zone decreases with increasing alkyl chain length of the dyes. In the turbidity zone a red shift of absorption maxima with

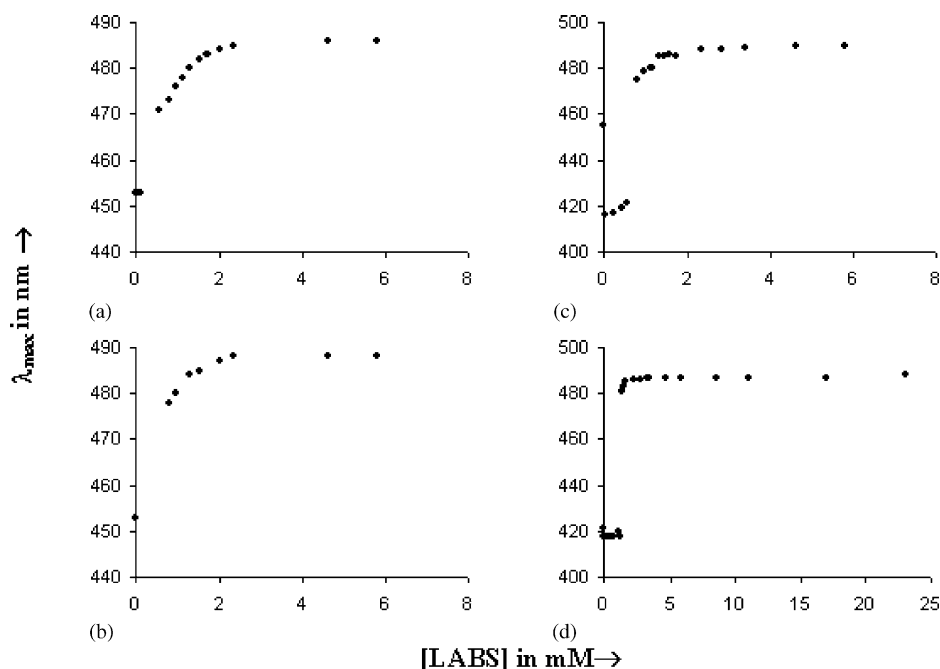


Fig. 2. Plot of [LABS] vs. λ_{\max} of: (a) C₃-NMe₂; (b) C₈-NMe₂; (c) C₁₂-NMe₂ and (d) C₁₈-NMe₂ dyes.

peak broadening is observed for C₁ and C₃ dyes. A shoulder at around 550 nm has been observed for C₃–C₆ dyes. For C₈ and C₁₀ dyes shoulders appear at 510 and 500 nm, respectively. The bathochromic shift in the turbid region may be attributed to the formation of J-type stacking of the dyes. Similarly, the hypsochromic band around 420 nm is due to the H-type of aggregation. Thus, in the turbid zone C₃–C₆ dyes remain in J-aggregated form, whereas C₈ and C₁₀ dyes remain both in H- and slip in J/H aggregated form [16]. With increasing [LABS], after turbidity zone, the dyes solubilize into the micelle as monomer. The dyes with alkyl chain longer than C₁₀ do not show any turbidity throughout the experimental concentration of LABS.

All dyes C₁–C₁₈ experience a relatively more non-polar environment in LABS micelle ($\lambda_{\max} = 482$ – 485 nm) as compared to AOS micelle ($\lambda_{\max} = 473$ – 485 nm). In complete micellized condition of LABS, with increasing hydrophobicity of the dye molecules, the λ_{\max} increases sharply from C₁–C₃ dye (482–486 nm) and remains almost constant (486–490 nm) up to C₁₄ dye. The decrease in λ_{\max} for C₁₆ and C₁₈ dyes up to 485 nm is assigned to the incompatibility of alkyl chain of the dyes with alkyl chain of LABS. Whereas, in AOS micelle the solubilization takes place up to C₁₆ dye, and C₁₈ dye remains in the bulk phase. By comparing the λ_{\max} values with $E_T(30)$ parameters in various solvents the probable solubilization site of dyes in various surfactants (above CMC) have been proposed (Table 4).

3.2. Emission spectra

All the dyes show emission maxima at 580–582 nm in the absence of surfactant. However, C₁₆ and C₁₈ dyes show λ_{em}

Table 4

The $E_T(30)$ value of the probable solubilization site of dyes in various surfactants (above CMC) obtained from λ_{\max} values

Dyes (C _n)	C ₁	C ₃	C ₅	C ₆	C ₈	C ₁₀	C ₁₂	C ₁₄	C ₁₆	C ₁₈
$E_T(30)$ AOS	56.9	53.1	52	52	52	52	51.1	51.1	51.1	50.6
LABS	52.4	51	49	49	49	49	48.4	48.4	50	50

at 582 nm with shoulder at 560 nm. The λ_{em} at 560 nm may be attributed to the fluorescence emission from the excited dimer species of the dyes, while the higher λ_{em} value may be due to the monomer species. Addition of AOS does not change the λ_{em} of C₁–C₁₄ dyes. But for C₁₆ and C₁₈ dyes on addition of AOS the shoulder at 560 nm vanishes and a peak appears at 577 nm up to 0.11 mM of AOS and then shifts to 581 nm. With increasing [AOS], it experiences a bathochromic shift up to 581 nm. The addition of LABS does not effect the λ_{em} of C₁–C₁₀ dyes. But for C₁₂–C₁₆ dyes a hypsochromic shift of about 3–4 nm is observed. Above the CMC, the λ_{em} value (582–584 nm) does not change for all dyes.

3.2.1. Fluorescence intensity

All the dyes show weak fluorescent bands in the absence of surfactant. On addition of AOS or LABS, the fluorescence intensity increases sharply and then attains maximum after a certain concentration of surfactant (Figs. 3 and 4).

In the presence of AOS (5.8 mM) the fluorescence intensity value of C₁–C₁₂ dyes is almost same and gradually decreases with increasing chain length of the dye (C₁₄–C₁₈). But in case of LABS, with increasing chain length of the dyes (from C₁–C₈) the intensity value increases from around 171 to 260 and after that remains constant up to C₁₄ dye, and then

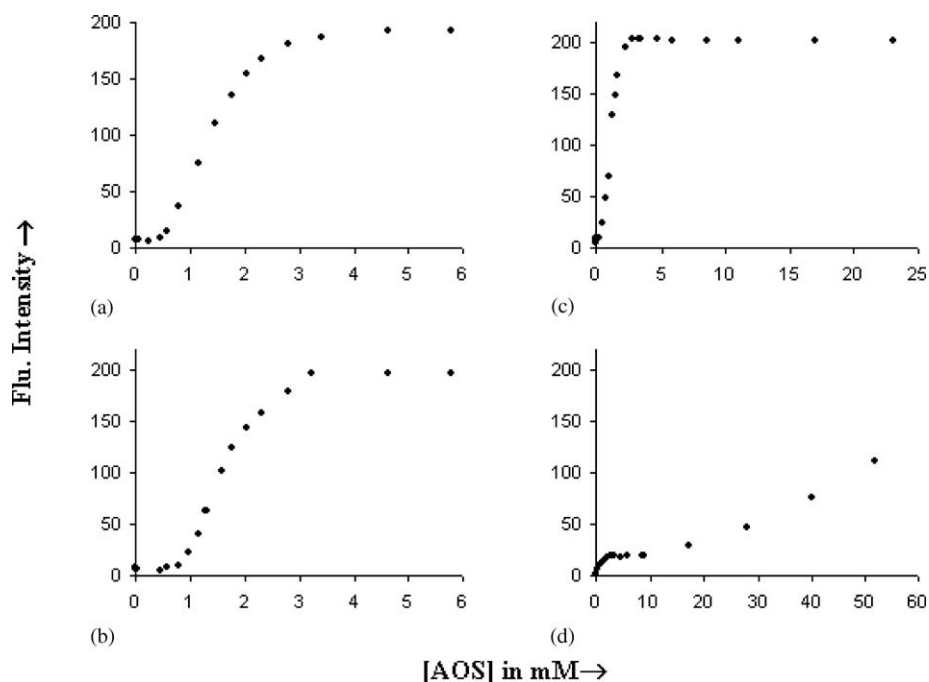


Fig. 3. Plot of [AOS] vs. fluorescence intensity of: (a) C₃-NMe₂; (b) C₈-NMe₂; (c) C₁₂-NMe₂ and (d) C₁₈-NMe₂ dyes.

again decrease to 112 for C₁₆ and C₁₈ dyes. The enhancement of the fluorescence intensity may be ascribed to the increase in rigidity of the dye molecule due to increase hydrophobic interaction with the surfactant. Conversely the decrease in intensity (C₁₆ and C₁₈ dyes both in AOS and LABS) may be due to the orientation of the dye chromophore, which remains away from the micellar interface. The large decrease in emission intensity for C₁₈ dye even up to 52 mM of AOS indicates the presence of dimeric form of the dye, which pre-

dominates over monomeric form as shown from absorption spectra.

The plots of [surfactant] versus emission intensity (Figs. 3 and 4) for all the dyes show S-type curve. Two break points at 0.5–0.9 and 1.78 mM of AOS are observed for C₁–C₁₂ dyes in AOS micelle. Similarly, for LABS micelle two break points at 0.8–1.3 and 1.7–2.06 are observed for all dyes. It is again seen that the lower break point value remains constant up to C₁₀ dye and gradually increases to

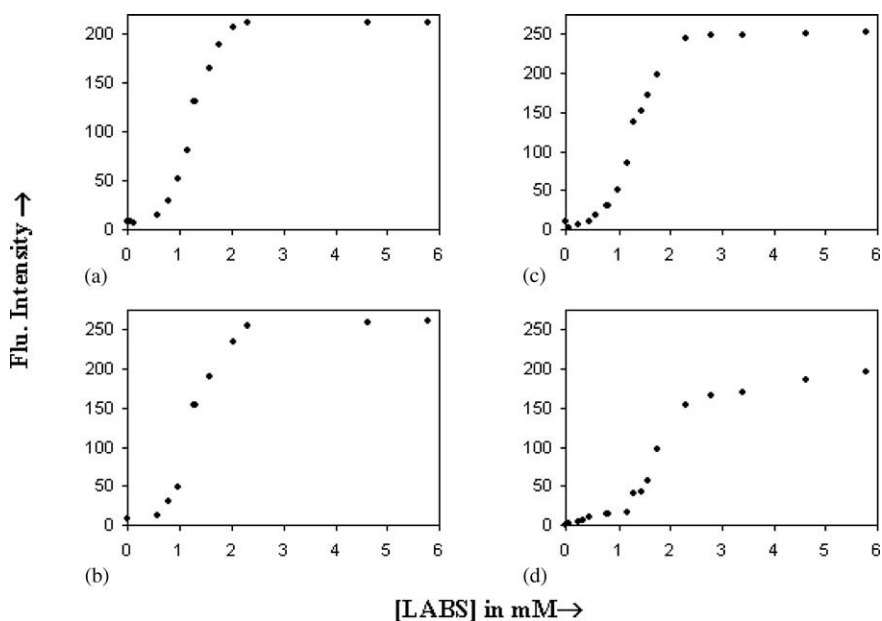


Fig. 4. Plot of [LABS] vs. fluorescence intensity of: (a) C₃-NMe₂; (b) C₈-NMe₂; (c) C₁₂-NMe₂ and (d) C₁₈-NMe₂ dyes.

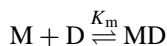
1.34 mM with increasing alkyl chain of the dye. However, the higher break point value initially decreases from C₁–C₃ and then remains constant up to C₁₂ dye and then attains a value of 2.06 for C₁₄–C₁₈ dyes. These lower break points may be referred to as critical aggregation constant (CAC) and the higher break point may be the CMC of the surfactant. The CMC of LABS has been reported to be 0.2 mM. An increase in CMC of LABS has also been reported by Nayyar and co-workers due to the presence of sodium oleate [17].

From the emission intensity the aggregation number of the surfactant AOS and LABS are calculated by using Eq. (1) [18].

$$\ln \frac{F_0}{F} = \frac{[Dye]N}{[s] - CAC}, \quad (1)$$

where F_0 and F are the intensities at CAC of surfactant and at individual [surfactant] ($[s]$) above CAC, respectively. N is the aggregation number. CAC for AOS and LABS are taken from the lower break points, i.e. 0.58 ± 0.2 and 0.84 ± 0.2 , respectively. The aggregation number for AOS and LABS are found to be 30 ± 3.2 and 36 ± 4.3 , respectively.

The binding constant K_m of the dyes which form a dye–micelle complex (MD) have been determined. By assuming that one dye molecule binds with one micelle:



The binding constant K_m is calculated by using Eq. (3).

$$I_t = \frac{I_w}{1 + K_m[M]} + \frac{I_m K_m[M]}{1 + K_m[M]} \quad (2)$$

and

$$K_m = \frac{I_t - I_w}{I_m - I_t} \times \frac{1}{[M]} \quad (3)$$

Here, I_t , I_w and I_m are the intensity at any [surfactant], in water and in micellized surfactant, respectively. The value of binding constant (K_m) for all the dyes in AOS and LABS are calculated and the plot of K_m versus C_n (number of carbon atom in the alkyl chain of the dye) is shown in Fig. 5. From the plot, it is observed that the binding of dye with surfactant increases up to C₆ dye in both the surfactant and then decreases.

The binding of cationic dyes having hydrophobic chains with anionic surfactant aggregates may be due to electrostatic interaction and hydrophobic interaction. The binding of dye up to C₆ with the surfactant seems to be due to both the interactions. Whereas, with increase in chain length the hydrophobic interaction dominates. Due to increase in hydrophobicity the dye molecules experience a pulling effect towards the micellar core, which destabilizes the binding species. Thus, the increase in hydrophobic group may experience a decrease in binding constant. The leveling up from C₈–C₁₂ dyes may be due to compatibility of alkyl chain of the dyes with that of the surfactants. Further decrease in binding constant

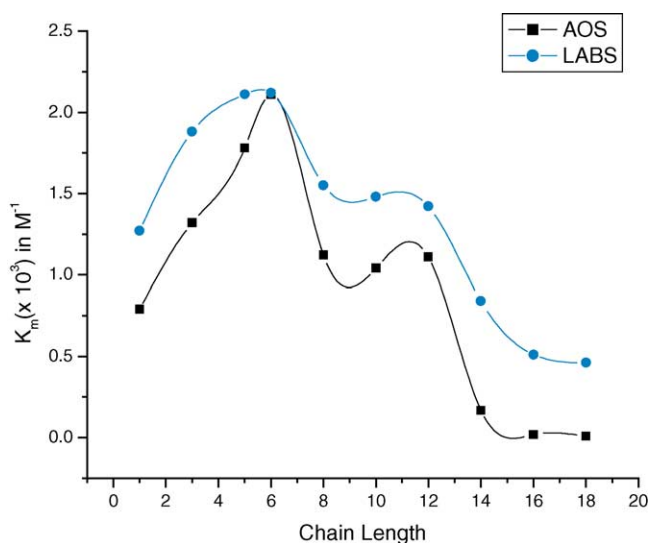


Fig. 5. Plot of binding constant of dye with [chain length] in LABS and AOS surfactant.

for C₁₆ and C₁₈ dyes may be attributed to the hydrophobic effect.

Acknowledgement

The authors thank to Department of Science and Technology, New Delhi and University Grants Commission, New Delhi for financial support through FIST and DRS project, respectively.

References

- [1] A.T. Katoh, Y. Inagaki, R. Okazaki, Bull. Chem. Soc. Jpn. 70 (1997) 1109, Bull. Chem. Soc. Jpn. 70 (1997) 2279.
- [2] A.S. Shetty, J. Zhang, J.S. Moore, J. Am. Chem. Soc. 118 (1996) 1019.
- [3] L.F. Vieira Ferreira, A.S. Oliveira, F. Wilkinson, D. Worrall, J. Chem. Soc., Faraday Trans. 92 (1996) 1217.
- [4] E.S. Emerson, M.A. Conlin, A.E. Rosenoff, K.S. Norland, H. Rodriguez, D. Chin, G.R. Bird, J. Phys. Chem. 71 (1967) 2396.
- [5] K. Shirota, K. Kajikawa, H. Takezoe, A. Fukuda, Jpn. J. Appl. Phys. 29 (1990) 750.
- [6] A. Mishra, R.K. Behera, P.K. Behera, B.K. Mishra, G.B. Behera, Chem. Rev. 100 (2000) 1891.
- [7] A. Mishra, S. Patel, R.K. Behera, B.K. Mishra, G.B. Behera, Bull. Chem. Soc. Jpn. 70 (1997) 2913.
- [8] A. Mishra, R.K. Behera, B.K. Mishra, G.B. Behera, J. Photochem. Photobiol. 121A (1999) 63.
- [9] A. Mishra, R.K. Behera, P.K. Behera, B.K. Mishra, G.B. Behera, J. Photochem. Photobiol. 116A (1998) 79.
- [10] S.S. Shah, M. Sallem Khan, H. Ullah, M. Ali Awan, J. Colloid Interface Sci. 186 (1997) 382.
- [11] A. Heindl, J. Strnad, H.H. Kohler, J. Phys. Chem. 97. (1993).
- [12] A.K. Sahaya, B.K. Mishra, G.B. Behera, D.O. Saha, Indian J. Chem. 27A (1988) 561.

- [13] J.K. Mishra, A.K. Sahaya, B.K. Mishra, *Indian J. Chem.* 30A (1991) 886.
- [14] A.K. Sahaya, B.K. Mishra, G.B. Behera, *Indian J. Technol.* 27 (1989) 89.
- [15] B.K. Mishra, M. Kuanar, A. Mishra, G.B. Behera, *Bull. Chem. Soc. Jpn.* 69 (1996) 2581.
- [16] S. Mohapatra, P.K. Behera, S. Das, B.K. Mishra, G.B. Behera, *Indian J. Chem.* 38A (1999) 815.
- [17] S. Das, N. Nayyar, R.G. Bhilrud, K.S. Narayan, V.V. Kumar, *J. Am. Oil. Chem. Soc.* 71 (7) (1994) 157.
- [18] G. Saroja, A. Samanta, *J. Chem. Soc., Faraday Trans.* 92 (1996) 2697.